

RESEARCH ARTICLE | JULY 06 2023

# One-way propagation of topologically non-conventional bulk transverse elastic waves in infinite and finite superlattices: Application to low-loss acoustic wave devices

Pierre A. Deymier   ; Keith Runge 

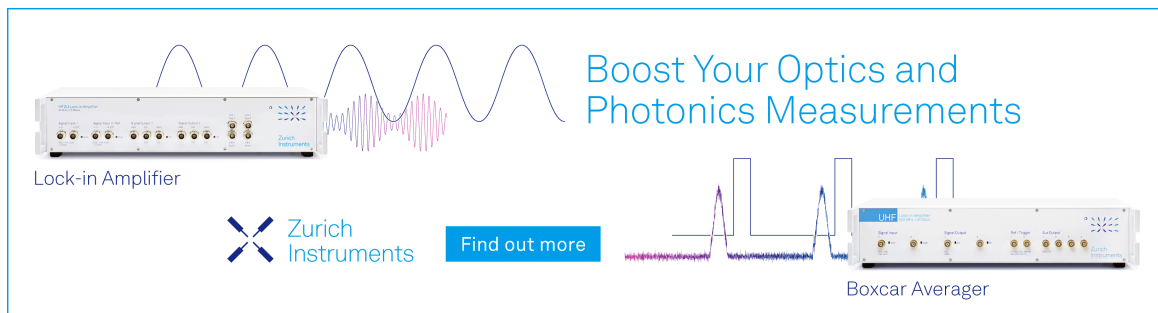
 Check for updates

*Appl. Phys. Lett.* 123, 012202 (2023)


<https://doi.org/10.1063/5.0156591>



Boost Your Optics and Photonics Measurements



Lock-in Amplifier



Find out more

Boxcar Averager

# One-way propagation of topologically non-conventional bulk transverse elastic waves in infinite and finite superlattices: Application to low-loss acoustic wave devices

Cite as: Appl. Phys. Lett. **123**, 012202 (2023); doi: [10.1063/5.0156591](https://doi.org/10.1063/5.0156591)

Submitted: 1 May 2023 · Accepted: 19 June 2023 ·

Published Online: 6 July 2023



View Online



Export Citation



CrossMark

Pierre A. Deymier<sup>a)</sup>  and Keith Runge 

## AFFILIATIONS

Department of Materials Science and Engineering, The University of Arizona, Tucson, Arizona 85721, USA

<sup>a)</sup>Author to whom correspondence should be addressed: [deymier@arizona.edu](mailto:deymier@arizona.edu)

## ABSTRACT

Static superlattices that do not break time-reversal symmetry can support robust topologically protected elastic waves with non-zero amplitude in the forward propagating direction but zero amplitude in the opposite direction. We form a prototypical acoustic wave device by sandwiching a finite superlattice that supports one-way propagating waves between input and detector layers. Compared to conventional elastic waves, topologically protected waves provide a significant benefit for reducing the return loss of the prototypical device. Superlattices supporting topologically protected acoustic waves provide attractive and disruptive solutions for designing the next-generation of low-loss acoustic wave devices for telecommunication or sensing.

Published under an exclusive license by AIP Publishing. <https://doi.org/10.1063/5.0156591>

Acoustic wave (AW) devices such as bulk acoustic wave (BAW), surface acoustic wave (SAW), and Love wave (LW) devices find many applications in radio frequency (RF) telecommunication<sup>1,2</sup> or sensing.<sup>3,4</sup> SAW and LW devices are constituted of an input transducer for transduction of a Rayleigh wave on the surface of a piezoelectric material or a Love wave in a thin film deposited on a piezoelectric substrate and an output transducer for detection. Transduction and detection typically use interdigital transducers (IDT). The fundamental reason why telecommunication relies on acoustic technology is that, for the same RF, the wavelength of acoustic waves is roughly a hundred thousand times smaller than the one of electromagnetic waves, enabling small footprints. AW devices for RF and sensing applications also exhibit very high-quality factors. However, the performance of AW devices is strongly affected by loss. Insertion loss is an important performance metric of AW devices. It is the ratio of power transmitted to the output transducers and the incident power. In part, insertion loss results from reflections that cause return loss, and in part by parasitic absorption. Return loss measures the amount of reflected signal caused by the mismatch between the impedance of the transduction regions of the device and that of the delay line region between the transducers. Return loss adversely affects the performance of acoustic RF devices and constitutes a major technical barrier in today's AW device

technology. The emerging field of topological acoustics provides fertile ground to address some of the technological challenges faced by current AW device technologies. In particular, the phenomenon of one-way propagation (i.e., immunity to backscattering) of topologically protected acoustic waves<sup>5</sup> may enable the design of AW devices with reduced return loss. Topological protection, potentially leading to immunity against scattering of an incident wave by a discontinuity in impedance, requires a counter-propagating wave that (1) is orthogonal to the incident wave or (2) has no amplitude (i.e., does not exist at all). The first case corresponds to topological edge/interface waves that conserve time-reversal symmetry.<sup>6</sup> Edge and interface states live at the surface of acoustic topological insulators or at interfaces between topological insulators with different topological characteristics. The second case corresponds to bulk waves that break time-reversal symmetry via, for instance, spatiotemporal modulation of the elastic properties of the wave-supporting medium.<sup>7,8</sup> Time-reversal-symmetry-preserved topological edge/interface waves are not robust against all types of scatterers. Only scatterers that cannot mix orthogonal waves will be invisible to the incident wave. Edge/interface waves may, therefore, not offer a robust solution to reducing return loss in AW devices. Furthermore, the integration of expansive topological insulating phononic structures that support edge/interface states into AW devices may challenge

device miniaturization. In the second case, the waves that break time-reversal-symmetry are more robust against backscattering. However, the physical realization of spatiotemporal modulation in, for instance, a piezoelectric medium<sup>9</sup> may be impractical or at best prohibitively costly for mass produced AW devices.

In this paper, we discuss the potential of topologically protected bulk elastic waves in superlattices, which do not require time modulations and may offer a path toward practical design of AW devices with low return loss. In the 1980s and 1990s, the focus of studies of elastic waves in superlattices was on their frequency gaps (i.e., Bragg gaps) or on localized modes at free surfaces or at interfaces in semi-infinite and finite superlattices.<sup>10–12</sup> Following more recent work on the topological properties of electromagnetic superlattices,<sup>13</sup> we discovered topologically protected elastic waves that propagate in static superlattices with non-zero amplitude in the forward direction but zero amplitude in the backward direction.<sup>14,15</sup> This discovery was overlooked and unheeded, but as we show here, it is not less important than that of topologically protected edge/interface or modulated acoustic waves for the design of future high performance AW devices. These topologically protected elastic waves do not possess the wider bandwidth that other topologically protected waves may possess; however, their narrow operational range of frequency may be advantageous when integrating with the current narrow band AW devices, such as filters for telecommunication applications. Inserting an appropriately designed superlattice between the IDTs in an acoustic RF device has the potential of reducing return loss. We note that the fabrication of superlattices in the form of Bragg gratings is a common feature in RF device manufacturing; however, these gratings are currently used for their reflection capabilities due to their bandgaps. A superlattice topological acoustic-based solution to reduce insertion/return loss in AW devices would be an attractive and disruptive innovation for industrial applications.

We first recall the topological and propagative properties of superlattices [Fig. 1(a)].

We focus on transverse waves with a displacement in the plane of the superlattice layers.<sup>11</sup> The displacement field in the infinite superlattice composed of two types of materials 1 and 2 takes the form of Bloch waves, namely,

$$u(x) = e^{iqx} u(q, x), \tag{1}$$

where the wave number  $q \in \left[-\frac{\pi}{L}, \frac{\pi}{L}\right]$ . The thicknesses of the alternating layers are  $d_1$  and  $d_2$ , respectively. The period of one unit cell of the

superlattice is  $L = d_1 + d_2$ . The periodic functions in the layers 1 and 2 in the  $n^{\text{th}}$  unit cell are given by

$$u_1(q, x) = e^{iqnL} \left( A_+ e^{ik_1(x-nL)} + A_- e^{-ik_1(x-nL)} \right), \tag{2a}$$

$$u_2(q, x) = e^{iqnL} \left( B_+ e^{ik_2(x-nL-d_1)} + B_- e^{-ik_2(x-nL-d_2)} \right), \tag{2b}$$

with  $k_1 = \frac{\omega}{c_1}$  and  $k_2 = \frac{\omega}{c_2}$ .  $A_{\pm}$  and  $B_{\pm}$  are the amplitude of the forward and backward propagating waves in media 1 and 2, respectively. The density and transverse speed of sound in the two types of materials are  $\rho_1, \rho_2$  and  $c_1, c_2$ , respectively. Using continuity conditions of the displacement and of the stress at the interfaces between layers 1 and 2 and using the transfer matrix method, we found the following dispersion relation:

$$\cos qL = \cos k_1 d_1 \cos k_2 d_2 - \frac{1}{2} \left( F + \frac{1}{F} \right) \sin k_1 d_1 \sin k_2 d_2 \tag{3}$$

and the amplitudes for layer 1 is

$$A_+ = \frac{1}{2} \left( F - \frac{1}{F} \right) \sin k_1 d_1 \sin k_2 d_2 + \frac{i}{2} \left( F - \frac{1}{F} \right) \cos k_1 d_1 \sin k_2 d_2, \tag{4a}$$

$$A_- = i \left[ \sin k_1 d_1 \cos k_2 d_2 + \frac{1}{2} \left( F + \frac{1}{F} \right) \cos k_1 d_1 \sin k_2 d_2 - \sin qL \right]. \tag{4b}$$

and for layer 2, it is

$$\begin{pmatrix} B_+ \\ B_- \end{pmatrix} = \frac{1}{2} \begin{pmatrix} (1+F)\alpha_1 & (1-F)\beta_1 \\ (1-F)\alpha_1 & (1+F)\beta_1 \end{pmatrix} \begin{pmatrix} A_+ \\ A_- \end{pmatrix}. \tag{5}$$

In layer 2, the amplitude  $A$  is purely imaginary. In layer 1, the amplitude  $A_+$  is complex, where  $\alpha_i = e^{ik_i d_i} = \frac{1}{\beta_i}$ . In Eqs. (4a), (4b), and (5),  $F = \frac{k_1 \rho_1 c_1^2}{k_2 \rho_2 c_2^2}$ .

In Fig. 2, we report the calculated band structure of the infinite superlattice and the real and imaginary parts of the amplitudes  $A_+$  and  $A_-$ . This calculation is done for a superlattice with  $\frac{d_2}{c_2} = 1.2 \frac{d_1}{c_1}$  and  $F = 2$ . These conditions are not particularly stringent, and many materials may be chosen to achieve the desired density and speed of sound. The thickness of the layers controls in part the frequency range of the band structure. These geometric parameters may be only limited by the fabrication techniques.

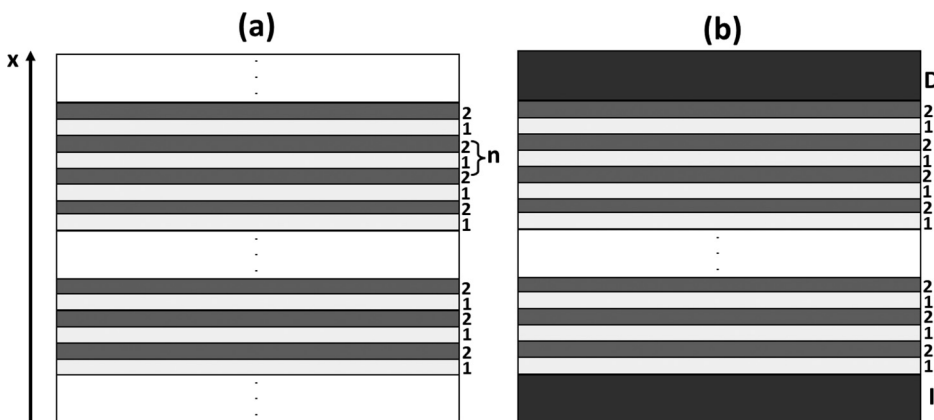
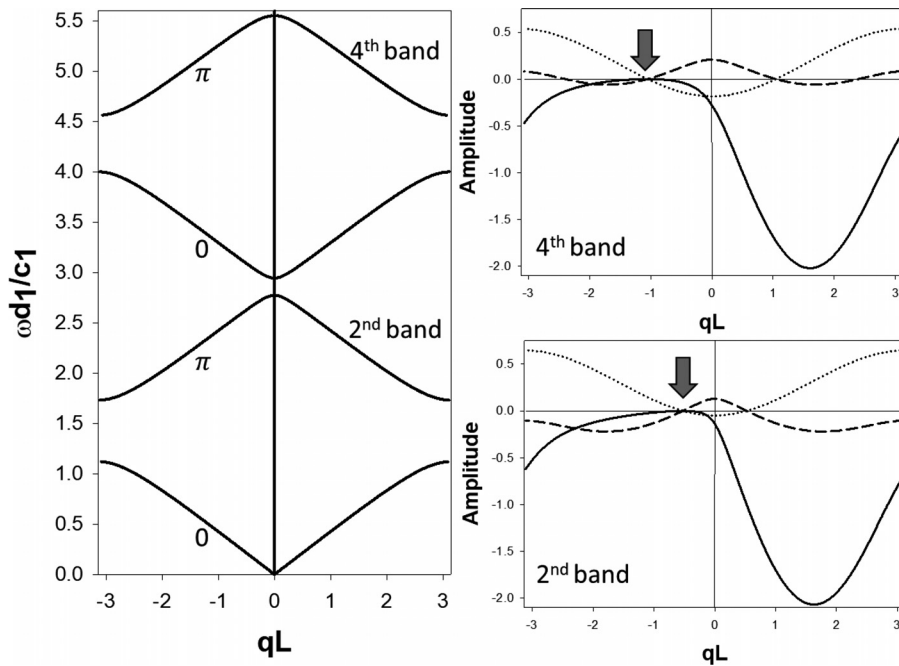


FIG. 1. Schematic representations of (a) the infinite superlattice composed of two types of layers 1 and 2 and (b) prototypical device composed of a finite size superlattice sandwiched between a layer, “I,” from which incident waves are emitted, and a layer “D” where transmitted waves are detected. The direction of propagation “x” is perpendicular to the layers.



**FIG. 2.** Left, band structure of the infinite super lattice with the physical parameters  $\frac{d_2}{c_2} = 1.2 \frac{d_1}{c_1}$  and  $F = 2$ . The geometric phase (Berry or Zak phase) accumulated by the elastic wave as one follows a closed path in  $qL$  space is indicated on the band structure. Bands 2 and 4 have a non-conventional topology with a geometric phase of  $\pi$ . The first and third bands correspond to conventional waves with 0 geometric phase. Right, real part (dotted line) and imaginary part (dashed line) of  $A_+$  and imaginary part (solid line) of  $A_-$  for transverse wave in the second band (bottom) and fourth band (top). The arrows mark the location where all amplitudes are zero.

We have shown<sup>14</sup> that if a band contains the frequency point,  $\omega_0$ , such that  $\sin k_2^0 d_2 = \sin \frac{\omega_0}{c_2} d_2 = 0$ , then the corresponding Berry phase (i.e., Zak phase or geometric phase over closed Brillouin zone) is equal to  $\pi$ . The second and fourth bands are topologically unconventional. At  $\omega_0(q_0)$ , the dispersion relation becomes  $\cos q_0 L = \cos(k_1 d_1 + k_2 d_2)$ ,  $A_+ = 0$  and  $A_- = i[\sin(k_1 d_1 + k_2 d_2) - \sin q_0 L]$ . Since  $k_1 d_1 + k_2 d_2 > 0$ , the sign of  $q_0$  determines whether  $A_-$  vanishes or not. In the case of Fig. 2, all the amplitudes of the waves for the second band,  $A_+$  and  $A_-$  (and the associated  $B_+$  and  $B_-$ ), are zero for negative  $q_0 L = -0.524$  but not all zero for positive  $q_0 L = 0.524$ . The same behavior is observed for the fourth band at  $q_0 L = \pm 1.048$ . The amplitudes for waves represented by conventional bands with zero Berry phase do not become all zero over the entire Brillouin zone. This is an example of a static superlattice supporting topologically protected elastic waves, whereby a forward propagating wave does not have a backward propagating counterpart. This robust topological protection against backscattering is achieved in a static superlattice that breaks inversion symmetry but more importantly does not break time-reversal symmetry. At the point  $\{\omega_0, q_0\}$ , the amplitude of the acoustic wave changes sign, which is directly related to the non-conventional topology of the bands with a geometric phase of  $\pi$ . This observation has been discussed extensively in the context of electromagnetic superlattices<sup>13</sup> and is readily extendable to acoustic waves.

We now investigate the behavior of a prototypical AW device containing a finite superlattice [see Fig. 1(b)]. The superlattice is sandwiched between an input layer “I” and a detection layer “D” with impedances that may differ from those of the materials 1 and 2. Material 1 is connected to the region “I,” and material 2 is connected to the “D” layer for the finite superlattice to be constituted of an integer number of complete unit cells. We calculate the transmission coefficient of the finite superlattice using transfer matrices, as is done in Ref. 16. In Ref. 16, however, the study focused on the existence of

frequency gap and never addressed the topological protection of waves. The transmission coefficient is given by

$$T = \frac{4 \frac{Z_D}{Z_I}}{\left(\frac{Z_D}{Z_I} b - \frac{Z_I}{Z_I} c\right)^2 + \left(d + \frac{Z_D}{Z_I} a\right)^2}, \tag{6}$$

where

$$\begin{aligned} a &= \frac{\lambda - \mu \sin N\theta}{2 \sin \theta} + \cos N\theta, \\ b &= \sigma \frac{\sin N\theta}{\sin \theta}, \\ c &= \zeta \frac{\sin N\theta}{\sin \theta}, \\ d &= -\frac{\lambda - \mu \sin N\theta}{2 \sin \theta} + \cos N\theta. \end{aligned}$$

In the preceding equations, we have

$$\begin{aligned} \lambda &= \cos k_1 d_1 \cos k_2 d_2 - F \sin k_1 d_1 \sin k_2 d_2, \\ \mu &= \cos k_1 d_1 \cos k_2 d_2 - \frac{1}{F} \sin k_1 d_1 \sin k_2 d_2, \\ \sigma &= \sin k_1 d_1 \cos k_2 d_2 + F \cos k_1 d_1 \sin k_2 d_2, \\ \zeta &= -\sin k_1 d_1 \cos k_2 d_2 - \frac{1}{F} \cos k_1 d_1 \sin k_2 d_2 \end{aligned}$$

and  $\cos \theta = \frac{\lambda + \mu}{2}$ .  $N$  is the number of unit cells in the superlattice. In Eq. (6),  $Z_1 = \rho_1 c_1$ ,  $Z_D$ , and  $Z_I$  are the impedances of the layers of type 1, detection, and input layers, respectively. The latter two impedances may represent the effect of input and detection IDTs.

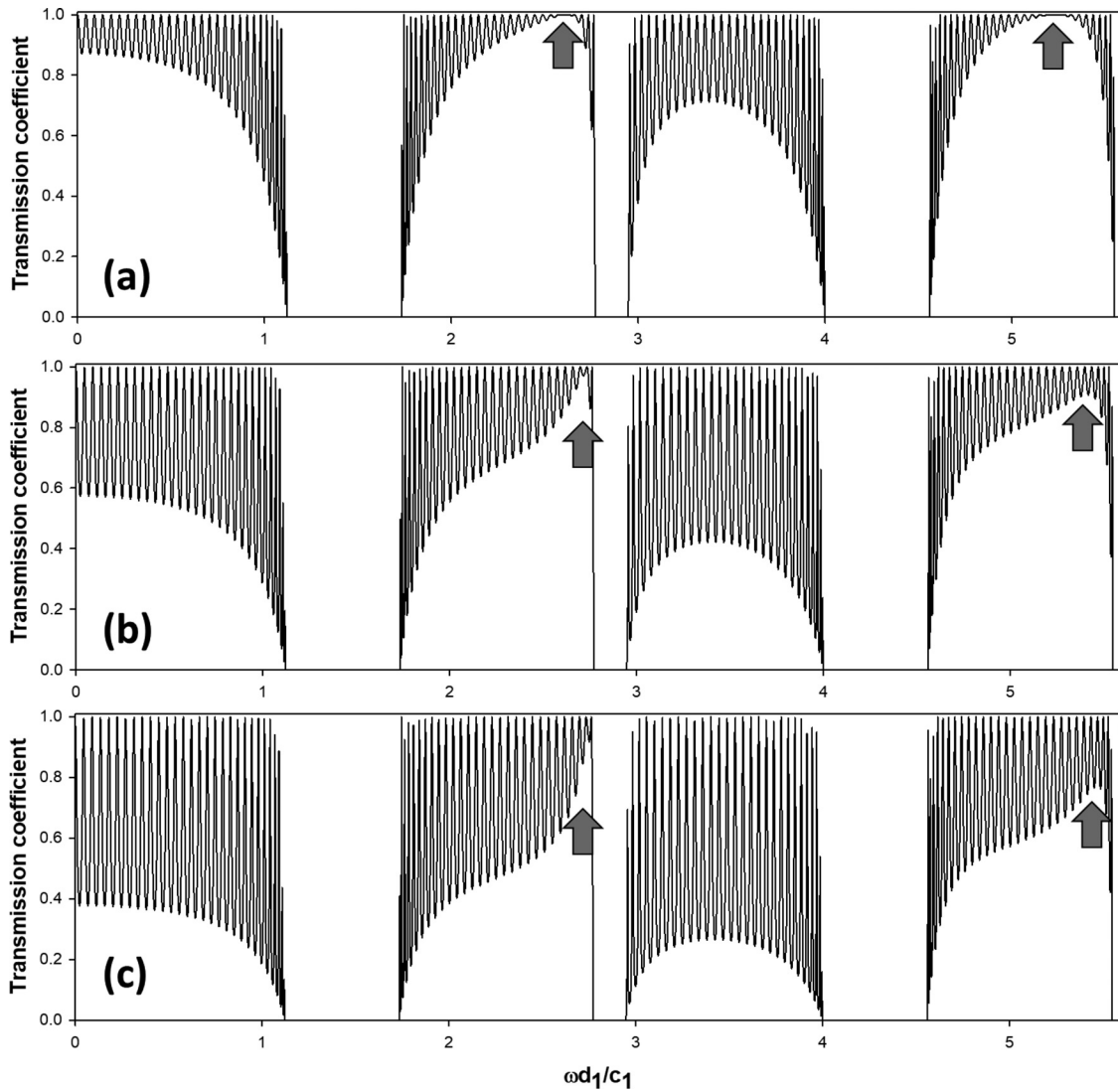


**FIG. 3.** Transmission coefficient,  $T$ , corresponding to the first four band of the finite superlattice with  $N = 30$  as a function of frequency for (a)  $Z_D = Z_I = Z_1$ , (b)  $Z_D = Z_I = 1.5Z_1$ , and (c)  $Z_D = Z_I = 2Z_1$ . The arrows indicate the location where topological protection leads to an increase in transmission.

In Fig. 3, we plot  $T(\frac{\omega}{c_1}d_1)$  for input and detection layers having the same impedance as the layer 1 and impedances exceeding that of the layer 1 by factors of 1.5 and 2. Each band supports 30 resonances corresponding to the number of periods of the finite superlattice. The lower envelope of the transmission coefficient of the topologically non-conventional bands (second and fourth) is asymmetric, while the first and third bands that have conventional topologies exhibit a standard more symmetrical behavior. We note in Fig. 3(a) that the lower envelope of the transmission coefficient of the second band is equal to one at  $\frac{\omega}{c_1}d_1 = 2.618$  (that is,  $k_2d_2 = 1.2 \times 2.618 = \pi$ , which corresponds to the condition  $\sin k_2d_2 = 0$ ). The amplitude of the backward propagating wave is zero under this condition. The same condition is satisfied for the fourth band  $\frac{\omega}{c_1}d_1 = 5.236$ , where  $k_2d_2 = 2\pi$ . When the input and detection layers possess higher impedances than layer 1, the frequency at

which topological protection occurs shifts toward the top of the second and fourth bands. Protection is not total as the lower part of the envelope of the transmission coefficient for the second band reaches a maximum of 1 in the case of Fig. 3(a),  $\sim 0.97$  in the case of Fig. 3(b), and  $\sim 0.91$  in Fig. 3(c). However, considering conventional waves in the third band, the lower envelope of the transmission reaches a maximum of  $\sim 0.71$  in case (a),  $\sim 0.42$  in case (b), and  $\sim 0.26$  in case (c). In terms of transmission coefficient, the return loss,  $RL$ , is defined as<sup>17</sup>

$$RL = -20 \log|T|. \quad (7)$$

We obtain  $RL = 0, 0.26$ , and  $0.82$  dB for the topologically protected wave in the second band as a function of the increasing impedance mismatch of Figs. 3(a)–3(c). For the optimum wave in the third band,

we obtain  $RL = 2.97, 7.53,$  and  $11.70$  dB. From a technological point of view, the last two cases exceed the recommended industry threshold value of 6 dB. The performance of the topologically protected wave in the fourth band is less than that of the second band but still significantly better than the performance of the conventional bands.

So far, we have discussed the performance of topologically protected bulk elastic waves in finite superlattices in terms of reduction of return loss. It is possible to consider a thin film cut out of the superlattice along a direction parallel to the  $x$  direction (i.e., film with surfaces perpendicular to the superlattice layers). For a suspended thin film superlattice, we must consider boundary conditions of stress-free surfaces. This type of condition has already been addressed<sup>11</sup> and simply multiplies the displacement given by Eqs. (2a) and 2(b) by a function representing the standing wave character of the wave in the direction of the film thickness. This solution does not affect the topological property of the waves along  $x$ . In the case of a thin film supported by a rigid substrate (approximating the configuration of a Love wave device), one needs to apply free-stress boundary condition on one side of the film and zero-displacement condition on the other side. These conditions will only affect the displacement field characteristics in the direction perpendicular to the film and again will not affect the topology of the wave along the  $x$  direction. Whether sagittal waves<sup>12</sup> exhibit the same non-reciprocity and topological immunity as transverse waves will be the subject of future work.

In summary, we have confirmed the existence of transverse elastic waves in an infinite superlattice that have non-zero amplitude when propagating in the forward direction but have zero amplitude when propagating in the opposite direction. These one-way propagating, topologically protected, waves are associated with elastic bands with non-zero Berry phase, and their existence does not require breaking time-reversal symmetry. We considered the transmission of the topologically protected waves through a prototypical AW device constituted of a finite size superlattice sandwiched between an input and a detection layer with different impedance than those of the superlattice constitutive materials. Topologically protected waves lead to a significant benefit for reducing the return loss of the device compared to elastic waves with conventional topology. The present study offers practical low-cost and industry compatible solutions for designing next-generation AW devices for telecommunication and sensing with reduced loss.

## AUTHOR DECLARATIONS

### Conflict of Interest

The authors have no conflicts to disclose.

### Author Contributions

**Pierre A. Deymier:** Conceptualization (equal); Writing – original draft (equal). **Keith Runge:** Conceptualization (equal); Writing – review & editing (equal).

## DATA AVAILABILITY

The data that support the findings of this study are available from the corresponding author upon reasonable request.

## REFERENCES

- R. Aigner, "SAW and BAW technologies for RF filter applications: A review of the relative strengths and weaknesses," in *IEEE International Ultrasonic Symposium Proceedings* (IEEE, 2008), p. 582.
- Y. Yang, C. Dejours, and H. Hallil, "Trends and applications of surface and bulk acoustic wave devices: A review," *Micromachines* **14**, 43 (2022).
- K. Länge, B. E. Rapp, and M. Rapp, "Surface acoustic wave biosensors: A review," *Anal. Bioanal. Chem.* **391**, 1509 (2008).
- M. I. Gaso Rocha, Y. Jiménez, F. A. Laurent, and A. Arnau, "Love wave biosensors: A review," in *State of the Art in biosensors-General Aspects*, edited by T. Rinken (IntechOpen, 2013).
- C. Rasmussen, L. Quan, and A. Alù, "Acoustic nonreciprocity," *J. Appl. Phys.* **129**, 210903 (2021).
- C. He, X. Ni, H. Ge, X.-C. Sun, Y.-B. Chen, N.-L. Lu, X.-P. Liu, and Y.-F. Chen, "Acoustic topological insulator and robust one-way sound transport," *Nat. Phys.* **12**, 1124 (2016).
- N. Swintek, S. Matsuo, K. Runge, J. O. Vasseur, P. Lucas, and P. A. Deymier, "Bulk elastic waves with unidirectional backscattering-immune topological states in a time-dependent superlattice," *J. Appl. Phys.* **118**, 063103 (2015).
- H. Nassar, X. C. Xu, A. N. Norris, and G. L. Huang, "Modulated phononic crystals: Non-reciprocal wave propagation and Willis materials," *J. Mech. Phys. Solids* **101**, 10 (2017).
- C. Croënne, J. O. Vasseur, O. Bou Matar, M.-F. Ponge, P. Deymier, A.-C. Hladky-Hennion, and B. Dubus, "Brillouin scattering-like effect and non-reciprocal propagation of elastic waves due to spatio-temporal modulation of electrical boundary conditions in piezoelectric media," *Appl. Phys. Lett.* **110**(6), 061901 (2017).
- E. H. El Boudouti and B. Djafari-Rouhani, "One-dimensional phononic crystals," in *Acoustic Metamaterials and Phononic Crystals*, Springer Series in Solid State Sciences Vol. 173, edited by P. A. Deymier (Springer, Berlin, 2013), Chap. 3.
- R. E. Camley, B. Djafari-Rouhani, L. Dobrzynski, and A. A. Maradudin, "Transverse elastic waves in periodically layered infinite and semi-infinite media," *Phys. Rev. B* **27**, 7318 (1983).
- B. Djafari-Rouhani, L. Dobrzynski, O. Hardouin Duparc, R. E. Camley, and A. A. Maradudin, "Sagittal elastic waves in infinite and semi-infinite superlattices," *Phys. Rev. B* **28**, 1711 (1983).
- M. Xiao, Z. Q. Zhang, and C. T. Chan, "Surface impedance and bulk band geometric phases in one-dimensional systems," *Phys. Rev. X* **4**, 021017 (2014).
- P. A. Deymier, K. Runge, and J. O. Vasseur, "Geometric phase and topology of elastic oscillations and vibrations in model systems: Harmonic oscillator and superlattice," *AIP Adv.* **6**, 121801 (2016).
- P. A. Deymier and K. Runge, *Sound Topology, Duality, Coherence and Wave-Mixing: An Introduction to The Emerging New Science of Sound*, Springer Series in Solid-State Sciences Vol. 188 (Springer, 2017).
- S. Mizuno and S.-I. Tamura, "Theory of acoustic-phonon transmission in finite-size superlattice systems," *Phys. Rev. B* **45**, 734 (1992).
- T. S. Bird, "Definition and misuse of return loss," *IEEE Antennas Propag. Mag.* **51**, 166 (2009).